Visual Communication Design Based on Sparsity-Enhanced Image Processing Models

Zheng Wang[1], Dongsik Hong[2]
College of Education Science, Henan Institute of Science and Technology, Xinxiang, China[1]
Pukyong National University, Busan Metropolitan, Korea[2]

***Abstract*—In the field of visual communication, image clarity and accuracy are the key to convey effective information. A new sparsity-enhanced image processing model is introduced to address the limitations of traditional image processing models in terms of image resolution and fidelity. This model combines a deep neural networks learning framework with a sparse convolutional neural networks enhancement module to complete image reinforcement processing, thereby achieving more accurate image reconstruction techniques. Dictionary learning is used to train models so that the sparse representation of low resolution and high-resolution images has the same dictionary coefficients. By comparing with the existing techniques Enhanced Super-Resolution Generative Adversarial Network, Wide Activation for Efficient and Accurate Image Super-Resolution, and Bicubic Interpolation, and the new model achieves an average peak signal-to-noise ratio of 32.9334 dB, which significantly outperforms the comparison group, respectively, with improvements of 1.9252 dB, 6.6509 dB, and 9.7297 dB, respectively. In addition, the new model demonstrates advantages in structural similarity and learning to perceive image block similarity, implying that it not only enhances the objective quality of the image, but also improves the subjective visual effect of the image. The improved resolution and fidelity of the output image confirms the model's superior performance in processing details and textures. This advancement not only improves the accuracy and efficiency of image processing techniques, but also provides strong technical support for the creation and dissemination of high-quality visual content, which is particularly suitable for application scenarios requiring high-precision visual displays, such as satellite image analysis, remote sensing detection and medical imaging.**

Keywords*—Deep neural networks; convolutional neural networks; sparsity; dictionary learning; image reinforcement processing

I. Introduction

In the digital era, the rapid development of image processing technology has brought new challenges and opportunities for visual communication design [1]. High-quality visual content can not only improve the efficiency of information dissemination, but also enhance the user experience [2, 3]. However, existing image processing techniques face the problems of high computational complexity and resource consumption when dealing with high-resolution images [4, 5]. Therefore, the research explores new methods for image feature extraction and reconstruction using sparse representation theory, which is committed to reducing the computational cost while maintaining or even improving the visual quality of images.

The research proposes a novel convolutional sparsity enhancement module, which can effectively extract key features from images and has good compression ability for redundant information in images. By combining with deep learning algorithms, a complex network model that can adaptively learn and abstract features from images is formed. The model is not only capable of generating high-quality dictionaries from high-resolution images, but also capable of constructing corresponding dictionaries for low-resolution images, and then realizing accurate reconstruction of high-resolution images through specific reconstruction strategies.

The innovation of the method lies in its extended application of the concept of sparsity. By embedding the concept of sparsity enhancement into the convolutional network, it not only enhances the sensitivity of the model to image details, but also improves the accuracy of feature extraction and the clarity of the reconstructed image. In addition, the convolutional sparsity enhancement module reduces the number of parameters of the model through rational design to accommodate the limitation of computational resources in practical applications.

The research helps to shorten the design cycle and enhance the iteration speed of the design by improving the efficiency of image processing, which further improves the outward expression of the image. The study is divided into six sections. Section II is a summary overview of the research related areas, Section III is the implementation of the proposed methodology of the study. Section IV is the validation as well as the testing of the proposed methodology of the study. Results and discussion is given in Section V and finally Section VI concludes the paper.

II. Related Works

Sparse representation theory is an important theory in the field of signal processing and applied mathematics, mainly about how to accurately represent signals with as few nonzero elements as possible. Sparse representation theory is widely used in many fields such as image processing, audio processing, machine learning, and data compression and so on. For example, in image processing, tasks such as image denoising, compression, and super-resolution reconstruction can be effectively performed by sparse representation. In machine learning, sparse representation can be used for feature selection and dimensionality reduction, which helps to improve the performance and efficiency of the algorithms. Cheng et al. proposed a joint statistical and spatial sparse representation scheme for the challenges of practical image classification, and the study proved that it outperforms the existing methods on FMD, UIUC, ETH-80, and YTC databases, and that it efficiently

overcomes the noise effects and adapts to the small-scale datasets [6]. Wang et al. proposed a hierarchical method using term sparsity to address the challenge of improving the efficiency of polynomial optimization, and the study proved that it effectively accelerated the solution process while maintaining the accuracy of the solution [7]. Xue et al. proposed an image domain method based on material sparsity for the accuracy of multi-material decomposition of monoenergy CT images and proved that this method improved the accuracy of voxel fraction on images and patient data, and optimized its image quality in clinical applications [8]. Anderson et al. proposed a projection model downscaling method by introducing sparsity into the downscaling basis for numerical prediction acceleration under highly nonlinear problems, and the study proved that the method significantly improves the computational efficiency and achieves a 1.5 times acceleration performance relative to the traditional method [9]. Wu et al. proposed a method using feature streaming to address deep neural network parameter redundancy, proposed the use of feature flow regularization (FFR) method to enhance structural sparsity, and the study proved that the method improves sparsity and meets or exceeds the effect of advanced pruning methods on CIFAR-10 and ImageNet datasets [10].

Image enhancement is a key technique in the field of computer vision and image processing, aiming to improve the visualization of an image through various algorithms to make the features in the image more visible, and thus facilitating observation by the human eye or analysis by automated systems. Image enhancement is usually not concerned with the absolute accuracy of an image, but rather focuses on enhancing the information that is most important for a particular application. Zou et al. proposed a night vision image enhancement method based on the fusion of data from infrared, RGB camera and LiDAR sensors to address the issue of operational risk in dark environments. The study proved that the method can accurately identify the location of obstacles, realize instant alarms in night operations and have a better detection performance [11]. Tang proposed a diversity-maximizing Makarov image enhancement method based on Simpson exponent for the detection of malicious behavior in encrypted traffic and achieved classification through CNN, and the study proved that the method significantly improved the classification accuracy under different balance degrees and effectively mitigated the generalization bias caused by the difference in the depth of the network [12]. Yang et al. proposed a nonlinear anisotropic diffusion system combined with time-delay regularization to construct a structure tensor for image enhancement and segmentation, and verified the effectiveness of the method by Galerkin's method [13]. Zhou et al. proposed an improved single-image defogging algorithm based on weighted guidance coefficients for the visibility degradation of outdoor images due to haze, and combined it with joint adaptive image enhancement, and the experimental The results show that the algorithm can effectively overcome image distortion and loss of detail information, and the efficiency exceeds that of the traditional dehaze algorithm [14]. Peng et al. proposed an attenuated image enhancement method with adaptive color compensation and detail optimization for color compensation and loss of local detail information in underwater image enhancement, and the study proved that the method can effectively enhance the contrast, detail information, and balance the color [15].

To summarize, the current development of image processing models shows unprecedented great potential, while sparsity enhancement greatly enriches the theory and methods of image processing from a unique perspective. With the advancement of technology, image enhancement plays an increasingly important role in maintaining and improving image quality. However, how to balance the relationship between processing efficiency and enhancement effect is still the focus of future research. Further optimization and innovative improvement of algorithms in the research will bring new development opportunities for the field, especially in terms of the breadth and depth of practical applications to be deepened and explored.

III. Construction of Sparsity-Based Enhanced Image Processing Model

The study begins with the design of a sparsity-enhanced convolutional module and its application to image enhancement for enhanced feature reconstruction of images. The construction of image enhancement processing model based on this sparsity-enhanced convolutional module generates corresponding dictionaries from high- and low-resolution images, and then realizes the accurate reconstruction of high resolution images through specific reconstruction strategies.

A. Sparsity-Enhanced Convolutional Module Construction

In the current era of high-dimensional data flooding, traditional image processing models are often computationally intensive due to the large number of parameters, susceptible to noise interference, and difficult to extract features quickly and accurately [16]. The study proposes a sparsity-enhanced convolution module in this context. By optimizing the convolution module, the model complexity is streamlined, and the computational resources are concentrated on the key features of the data, thus effectively enhancing the stability and accuracy of signal processing. In addition, the sparsity-enhanced convolution module also enhances the interpretability of the model due to its simplicity, which is crucial for the requirement of algorithm credibility in practical application scenarios [17]. For this convolution module, the sparse representation of the image itself is first extracted and then the extracted sparse representation is further utilized to enhance the image reconstruction. It is first assumed that the given training set is shown in Eq. (1).

$$\left\{h_i \in \square^{m}, v_i \in \square^{l}\right\}_{i=1}^{n} \tag{1}$$

Based on this training set, sparse coding needs to be further satisfied by the corresponding dictionaries $D \coloneqq \left[d_1, d_2, \cdots, d_k\right]$ as well as $F \coloneqq \left[f_1, f_2, \cdots, f_k\right]$ in Eq. (2).

$$\begin{cases} \min\limits_{D,P,\left\{\phi_i^{h/v}\right\}_{i=1}^{n}} \sum\limits_{i=1}^{n}\left\{\frac{1}{2}\left\|h_i - D\phi_i^{h}\right\|_2^2 + \lambda\left\|\phi_i^{h}\right\|_p + \frac{1}{2}\left\|v_i - F\phi_i^{v}\right\|_2^2 + \lambda\left\|\phi_i^{v}\right\|_p\right\} \\ s.t. D \in \varsigma(m,k), F \in \varsigma(l,k), 0 \le p \le 1 \end{cases} \tag{2}$$

In Eq. (1) and Eq. (2), h_i denotes low-resolution image, v_i denotes high-resolution image, ϕ denotes sparse coding, $\left\|\phi_i^h\right\|_p$ denotes sparsity, and $\lambda \in \square^+$ denotes weighting of sparsity. In order to avoid the scale blurring problem of D and F during sparse coding, $\varsigma(a,b)$ should satisfy Eq. (3) [18].

$$\begin{cases} \varsigma(a,b) := \left\{ D \in \square^{a\times b} \middle| rand(D) = a \right. \\ a > b, \left\|d_i\right\|_2 = 1 \end{cases} \tag{3}$$

For sparsity in Eq. (2), it is usually measured using the l_1 norm, and the sparse coding of a given signal x over the dictionary D can be found by Eq. (4).

$$\phi^+ = \arg_\phi \min \left\|h - D\phi\right\|_2^2 + \lambda \left\|\phi\right\|_1 \tag{4}$$

It can be seen by Eq. (4) that $h = D\phi_h$ denotes the ideal low resolution image and $v = F\phi_v$ denotes the ideal high resolution image. By slightly modifying the notation, the sparse solution of the dictionary D and the sparse solution of the dictionary F can be expressed as shown in Eq. (5).

$$\begin{cases} \phi_{h_i}(D) : h_i \to \phi_{h_i} \\ \phi_{v_i}(F) : v_i \to \phi_{v_i} \end{cases} \tag{5}$$

Unlike conventional sparse coding, the sparsity-enhanced convolution module proposed in the study directly processes the whole image instead of processing the image in chunks. This approach avoids the edge effects and seam problems that may result from chunking, and ensures the global coherence and integrity of the image content. Specifically, in the proposed convolutional sparse coding module, each layer is implemented with an independent convolution operation, and these convolutional layers not only extract features of the image, but also enhance the sparse representation of these features layer by layer. In each iteration, the image is processed through a convolutional filter to extract features and apply a nonlinear activation function to enhance sparsity. Subsequently, the difference between the current sparse representation and the original image is evaluated by a loss function to guide the feature extraction and sparse enhancement in the next iteration layer. This iterative process continues until a preset sparse representation accuracy or an upper limit on the number of iterations is reached, and the final output of the enhanced sparse feature map provides a high-quality feature representation for subsequent image processing tasks. The study further employs a linear transformation to ensure the consistency of the sparse representation of the source image and the target image, which is shown in Eq. (6).

$$\phi_{v_i}(F) = A\phi_{h_i}(D) + \eta_i \tag{6}$$

In Eq. (6), η_i denotes the error. After obtaining the sparse representation of the low-resolution image, it is further enhanced to obtain enhanced sparsity by linear transformation. The convolutional sparse coding module as well as the linear transformation module are shown specifically in Fig. 1.

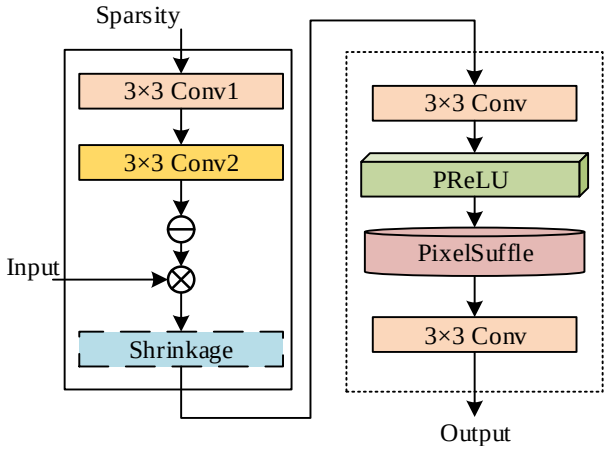

Fig. 1. Schematic diagram of the linear conversion strengthening module.

Eventually, the structure of sparsity-enhanced convolutional modules constructed by the study is shown in Fig. 3. The structure is designed to highlight the modularity, in which the number of each reinforcement module is not fixed but dynamically adjusted according to the required magnification to meet the precise control of different resolution enhancement requirements. This design allows the model to be flexibly adapted to a variety of magnification tasks, be it slight magnification or multiple magnification, ensuring that the image quality is guaranteed.

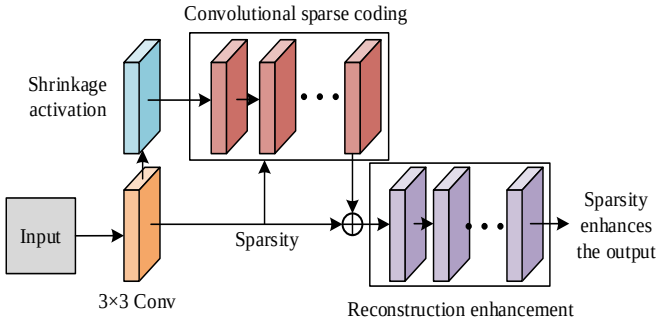

Fig. 2. Sparsity enhanced convolutional module structure diagram.

In Fig. 2, the convolutional kernel sizes used in the network are all. Choosing an appropriate convolutional kernel size can effectively balance the breadth of the sensory field with the local sensitivity of feature extraction, and thus optimize the model performance. In summary, the sparsity-enhanced convolutional module structure shown in Fig. 2 utilizes the flexibility in the number of its modules and the precise configuration of the convolutional kernel sizes to work together on the image processing task in order to achieve highly customized and optimized image magnification and feature enhancement results. Since conventional neural networks suffer from the problem of enhanced image smearing after processing the image, an anti-loss discriminator network module is further introduced to improve the problem. The structure of the adversarial loss discriminator module is specifically shown in Fig. 3.

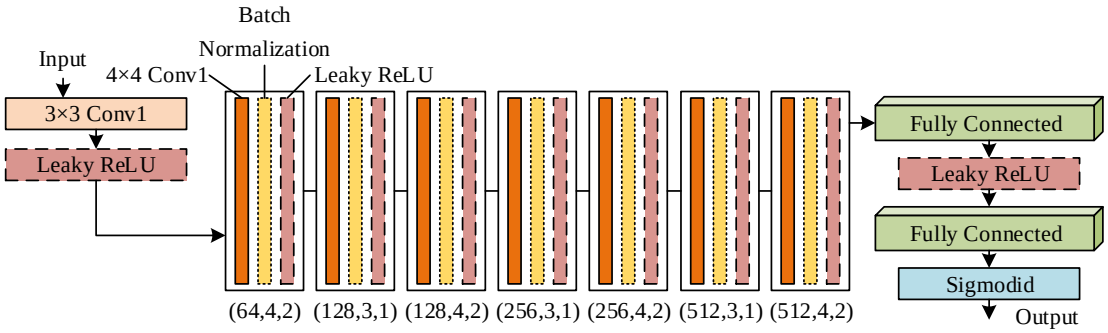

Fig. 3. Schematic diagram of counter loss discriminator module.

The introduced adversarial loss discriminator module is shown in Fig. 3, through which the batch normalization as well as the fully connected layer is introduced to effectively enhance the final image processing by further processing the sparsity in order to avoid the problem of severe smearing of the image.

B. Enhanced Image Processing Model Construction

Based on the constructed sparsity-enhanced convolutional model, let Y denote a low-resolution image that needs to be enhanced, and X denote an enhanced high-resolution image, then the relationship between them can be expressed as shown in Eq. (7).

$$Y = DownHX + n \tag{7}$$

In Eq. (7), $Down$ denotes down sampling, H denotes fuzzy matrix, and n denotes additive noise. The goal after combining the sparse representation is to approximate X by the dictionary D. For a data sample x_j, its sparse representation vector a_j. Then for the sparse representation matrix A, which is shown in Eq. (8).

$$\begin{cases} A = \min\limits_{A} \left(\|A\| \right)_0 \\ s.t. X \approx DA \end{cases} \tag{8}$$

In Eq. (8), $\|\cdot\|_0$ denotes the pseudo-paradigm number, which is set to the number of non-zero elements of A, and $X \approx DA$ is replaced by a fault-tolerant constraint form, as shown in Eq. (9).

$$\left(\|X - DA\| \right)_2^2 \le \varepsilon \tag{9}$$

In Eq. (9), ε denotes the BER threshold. The optimization of pseudo-paradigm belongs to the $NP-hard$ problem, by minimizing the number of paradigms, the sparsity can be effectively reduced to represent the sparsity, so the model will be rewritten as shown in Eq. (10).

$$\begin{cases} A = \min\limits_{A} \left(\|A\| \right)_1 \\ s.t. \left(\|X - DA\| \right)_2^2 \le \varepsilon \end{cases} \tag{10}$$

Then, the sparse representation coefficients lifting as well as the dictionary need to be estimated as shown in Eq. (11).

$$\left(A^{'}, D^{'} \right) = \arg_{A,D} \min \left(\|X - DA\| \right)_2^2 + \lambda \|A\|_1 \tag{11}$$

In Eq. (11), a data fitting term as well as a regularization term are included, and λ denotes the penalty parameter. In image enhancement processing, the extraction of visual features is carried out first, and the extraction process of visual features is specifically shown in Fig. 4.

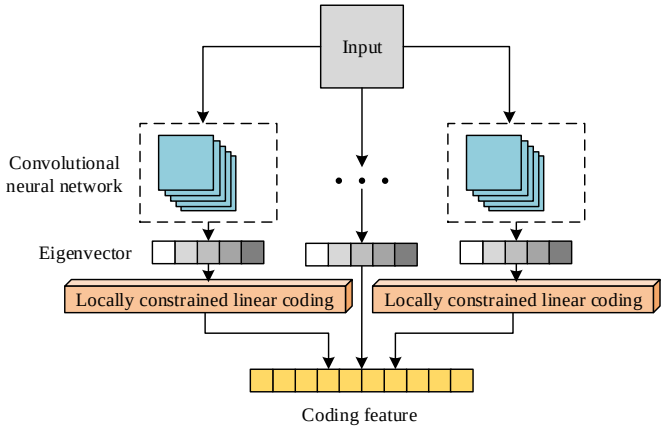

Fig. 4. Schematic diagram of the extraction process of visual features.

The VGG16 deep convolutional network trained on the ILSVRC-2012 dataset is chosen as the feature extractor, and for an image of size 224×224, the dimension of the extracted feature vector f_i is 4096. After obtaining the feature vector, the features are encoded by locally constrained linear coding. Firstly, a codebook is created and the set of feature vectors is divided into M clusters using the K-means clustering algorithm, and then a codebook is created at $B = \left[b_1^T, \cdots, b_M^T \right]$, where b_i denotes the center of mass of the i cluster. Then based on the codebook, each feature vector is encoded [19]. Let the extracted N the D dimensional feature vector be $F = \left[f_1^T, \cdots f_M^T \right]$, then the set of code words $\dot{F} = \left[\dot{f}_1^T, \cdots, \dot{f}_M^T \right]$ corresponding to F is searched by the condition of Eq. (12).

$$\min_{B}\sum_{i=1}^{N}\left\| f_i - B\dot{f}_i \right\|^2 + \lambda\left\| d_i * \dot{f}_i \right\|^2 \tag{12}$$

In Eq. (12), * denotes the element-level multiplication operation, B denotes the codebook, λ denotes the regular term coefficients, and d_i denotes the local adjustment variables. Then d_i can be expressed as shown in (13).

$$d_i = \exp\left(\frac{dist\left(f_i, B\right)}{\sigma}\right) \tag{13}$$

In Eq. (13), $dist\left(f_i, B\right) = \left[dist\left(f_i, b_1\right), dist\left(f_i, b_2\right), \cdots, dist\left(f_i, b_M\right)\right]^T$, $dist\left(f_i, b_j\right)$ denote the Euclidean distance between f_i and b_j and σ denotes the weight descent rate control parameter. For dictionary learning, a pair of high resolution as well as low resolution blocks are set to $P = \left\{p_h^k, p_l^k\right\}_k$. The main objective of dictionary learning is to train for this block so that the dictionary coefficients for sparse representation of low resolution as well as high resolution images are same. The sparse representation model for low resolution features is shown in Eq. (14) [20].

$$p_l = D_l A \tag{14}$$

In Eq. (14), p_1 denotes a low-resolution image block, D_l denotes a low-resolution dictionary, and A denotes the sparsity factor. For D_l, the K-SVD dictionary training method is used for calculation, as shown in Eq. (15).

$$\begin{cases} D_l = \arg_{D_l, A^k}\min\sum_k \left\| p_1^k - D_l A^k \right\|^2 \\ s.t. \left\| A^k \right\|_0 \le L \end{cases} \tag{15}$$

In Eq. (15), L denotes the maximum sparsity. If the sparse representation sparsity of the high resolution and low-resolution image block is the same, the sparse representation of the high resolution image block is specifically shown in Eq. (16).

$$D_h = \arg_{D_h}\min\sum_k \left\| p_h^k - D_h A^k \right\|_2^2 \tag{16}$$

This is then solved by the pseudo-inverse matrix as shown in Eq. (17).

$$D_h = p_h A^T \left(AA^T\right)^{-1} \tag{17}$$

For high- and low-resolution learning training, the process is shown in Fig. 5, which is mainly based on visual depth features in order to generate dictionaries of corresponding resolutions.

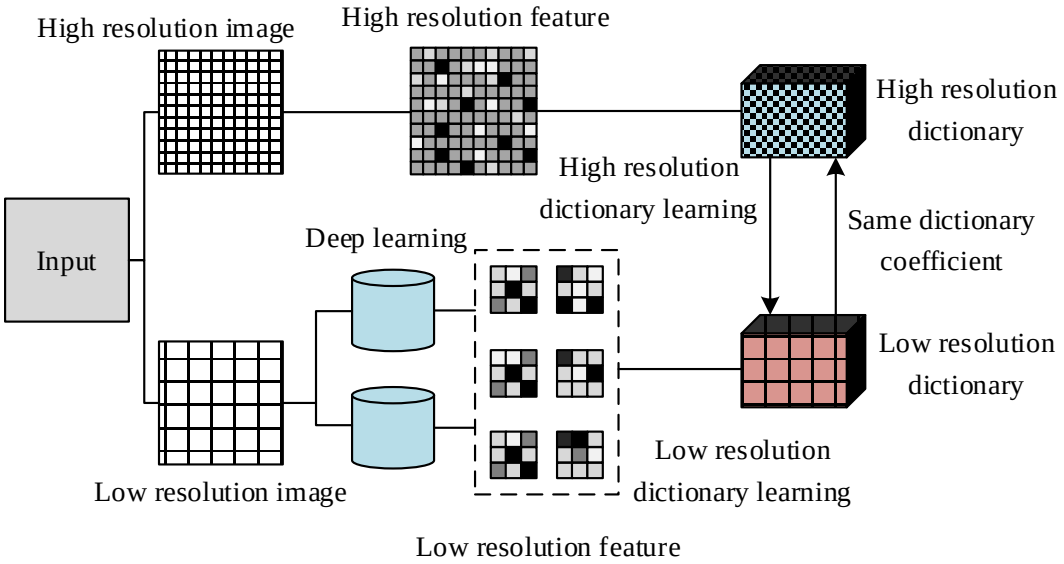

Fig. 5. Schematic of training for high- and low-resolution dictionary learning.

For the enhanced reconstruction processing of high-resolution images, based on the features extracted above, the features are multiplied with the projections obtained by dictionary learning to obtain the low resolution features p_l^k. Then p_l^k is encoded using the orthogonal matching tracking algorithm as shown in Eq. (18).

$$\begin{cases} A^k = \arg_{A^k}\min\sum_k \left\| p_l^k - D_l A^k \right\|^2 \\ s.t. \left\| A^k \right\|_0 \le L \end{cases} \tag{18}$$

Then, by multiplying its sparse representation sparsity with the high-resolution dictionary D_h, a more approximate high-resolution image block can be restored, as shown in Eq. (19).

$$p_h^k = D_h A^k \tag{19}$$

As shown in Fig. 6, the complete process of image super-resolution reconstruction is demonstrated, and the key technical link in this process is the sparsity-enhanced convolution-based module. The advantage of this module is that it can directly carry out one-time feature extraction for low-resolution images and realize the reconstruction of high-resolution images on this basis. In traditional super-resolution methods, multiple feature extraction and up sampling steps are often unavoidable, and each step may introduce noise or cause loss of information, thus affecting the clarity and texture of the final image.

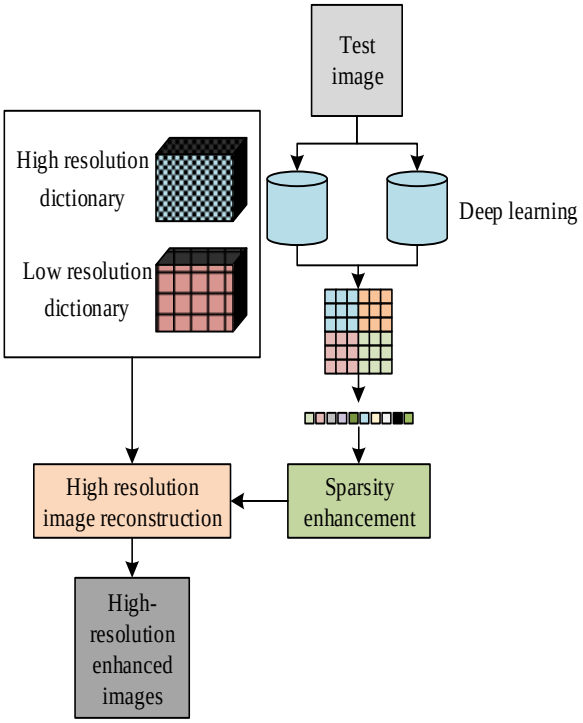

Fig. 6. Schematic diagram of image super-resolution reconstruction process.

With the sparsity-enhanced convolutional module, the low-resolution image first passes through a feature extraction layer that uses a well-designed convolutional kernel to refine the essential features and texture information in the image. These features are then processed through a sparsity enhancement layer, which utilizes the sparsity principle to further filter and highlight meaningful signals while suppressing unnecessary redundant information. The sparsity-enhanced features not only retain the key visual information of the image, but also enhance the expressiveness of the features, laying a solid foundation for the next reconstruction steps. Thereafter, the reconstruction module maps these enhanced features to the high-resolution space. In this process, up-sampling techniques such as interpolation, transpose convolution, etc. can be employed to recover the high-resolution structure of the image. Finally, a fine-tuning layer optimizes the reconstructed image to eliminate possible artifacts, enhance naturalness, and ensure that the resulting high-resolution image is visually as close as possible to the real HD image. Through such an efficient and integrated process, the image super-resolution reconstruction is not only computationally more efficient, but also more effective, resulting in accurate recovery of image details and significant improvement in overall quality.

IV. Testing of Sparsity-Enhanced Image Processing Models

To test the sparsity-enhanced image processing model proposed in the study, a more balanced hardware is required to perform the corresponding tests, considering the deep learning model used in it. To avoid the impact of hardware performance on the experiments, the study chose to use a cloud server platform for the tests, considering cost constraints and affordability. The DIV2k, Set5, and Set14 datasets are used for testing, and the DIV2K dataset is a benchmark dataset for image super-resolution that contains 2,000 high-quality 2K-resolution images; Set5 is a small dataset of five high-resolution images, which is often used for testing and validating super-resolution algorithms; and Set14 is like Set5, which contains 14 different images. Set14 contains 14 high-resolution images of different subjects and is also used to evaluate the performance of super-resolution algorithms. Bicubic Interpolation (BI) image enhancement method, Wide Activation for Efficient and Accurate Image Super-Resolution (WDSR) and Enhanced Super-Resolution Generative Adversarial Network (EGRAN) were selected for the study. Super-Resolution Generative Adversarial Networks (ESRGAN) are compared with the Sparsity intensifies image processing model (SIIP) proposed by the Institute. As shown in Table I, the details of hardware and software and model parameters used in the institute.

TABLE I. Software and Hardware Details and Model Parameter Settings

Hardware			Software	
Name	Supplier	Details	Ubuntu Server	20.04 LTS
Cloud server	AWS		TensorFlow	2.8.0
Instance type	p3.2xlarge		PyTorch	1.10.0
VCpu	Intel	8	CUDA	11.2
GPUs	Nvidia	Tesla V100	cuDNN	8.1.0
RAM	61GiB		Python	3.8.5
MEM	EBS	500GB	Jupyter Notebook	6.4.5

Parameter setting					
Name	Details	Name	Details	Name	Details
Filters	64	lambda (Greek letter Λλ)	0.01	β1	0.0
Kernel_size	3x3	Pool_size	2x2	β2	0.999
Strides	1	Units	1024	Batch Size	32
Padding	'same'	Optimizer	Adam	Epochs	20
Activation	ReLU	Learning_rate	1e-4	Early Stopping	Patience = 10

The Peak Signal-to-Noise Ratio (PSNR) and Structural Similarity (SSIM) of the four models are tested and the results are shown in Fig. 7. From Fig. 7(a), the proposed SIIP model possesses the best PSNR value. The high PSNR value of the SIIP model indicates that it retains a lot of details and structural information in the recovered image and reduces the noise and distortion, which is usually indicative of clearer and more accurate image recovery results. As can be seen in Fig. 7(b), the

proposed SIIP model of the study possesses the best SSIM values. The high score of the SIIP model on SSIM indicates its excellent ability to maintain the texture and structure of the image locally, especially when recovering the image, and to preserve its natural visual characteristics and consistency.

Ten images are selected to test the PSNR as well as SSIM of the four models in practical applications and the test results are shown in Fig. 8. From Fig. 8(a), the proposed SIIP model has the best PSNR value performance on all image processing, which indicates that the proposed SIIP model can output clearer results on image enhancement. From Fig. 8(b), the proposed SIIP model has the highest SSIM value performance on all the images, which indicates that the output image of the proposed SIIP model has the best fidelity, and it is able to achieve high resolution enhancement of the image without loss of image details.

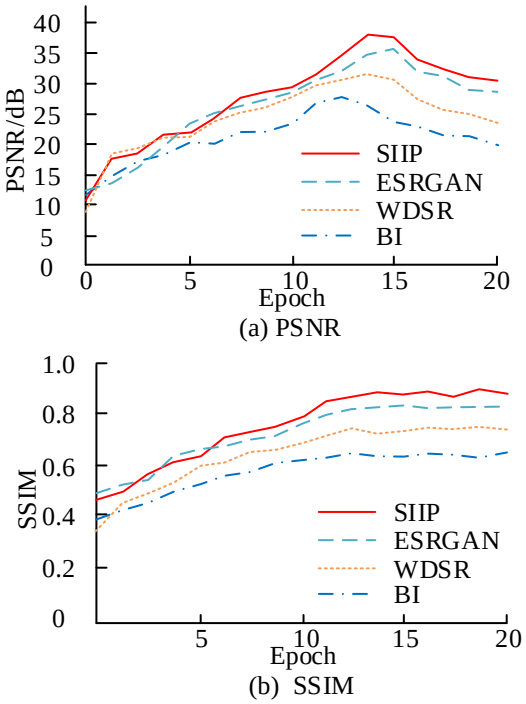

Fig. 7. Iterative performance testing of PSNR and SSIM for four models.

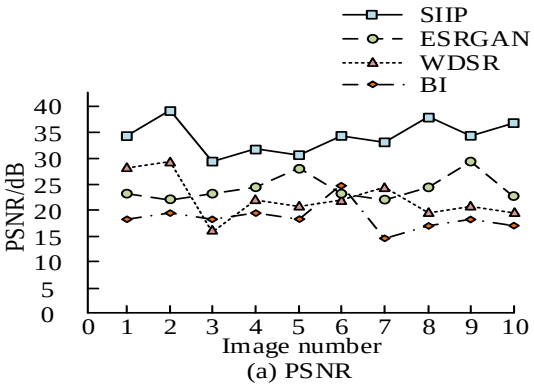

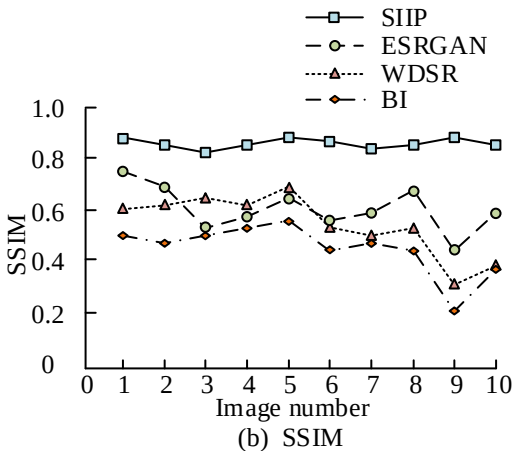

Fig. 8. PSNR and SSIM in image testing for four models.

The average performance of the four models at 2x zoom is tested, and the test metrics include PSNR, SSIM and Learned Perceptual Image Patch Similarity (LPIPS). The test results are shown in Table II. As can be seen from Table II, the average PSNR value of the proposed SIIP model reaches 32.9334 dB, which is 1.9252 dB, 6.6509 dB and 9.7297 dB ahead of the ESRGAN, WDSR, and BI models, respectively, and the average value of SSIM of the SIIP model is ahead of the other three models, and the value of LPIPS is also ahead of the other three models. Three models also showed the same lead. This result shows that the proposed SIIP model has better image enhancement performance and stronger image fidelity.

The response times of the four models at different magnifications are tested and the results are shown in Table III. From Table III, the average response time of the SIIP model proposed by the institute is 0.82 s, which is 4.99 s, 9.45 s and 18.30 s ahead of ESRGAN, WDSR and BI models, respectively.

TABLE II. AVERAGE PERFORMANCE TEST RESULTS OF THE FOUR MODELS AT 2X MAGNIFICATION

Algorithms	Index	Data set			Average
		DIV2k	Set5	Set14	
SIIP	PSNR	32.7811	33.2371	32.7821	32.9334
	SSIM	0.8621	0.8792	0.8914	0.8775
	LPIPS	0.0231	0.0124	0.0167	0.0174
ESRGAN	PSNR	30.2943	30.8762	31.8541	31.0082
	SSIM	0.8152	0.8064	0.8169	0.8128
	LPIPS	0.0672	0.0729	0.0861	0.0754
WDSR	PSNR	26.2356	27.3267	25.2854	26.2825
	SSIM	0.7561	0.7152	0.7217	0.7310
	LPIPS	0.0891	0.0998	0.0826	0.0905
BI	PSNR	22.2366	23.4371	23.9374	23.2037
	SSIM	0.6273	0.5964	0.6342	0.6193
	LPIPS	0.1274	0.1102	0.0998	0.1124

TABLE III. RESPONSE TIME TESTS OF FOUR MODELS AT DIFFERENT MAGNIFICATIONS

Data set	Magnification	Response time/s			
		SIIP	ESRGAN	WDSR	BI
DIV2k	2	1.9	9.2	15.7	25.9
	3	1.7	8.7	14.2	24.1
	4	1.5	7.1	13.1	22.7
Set5	2	0.4	4.9	8.6	17.1
	3	0.4	4.1	7.2	16.5
	4	0.3	3.8	7.1	13.7
Set14	2	0.5	5.3	9.8	18.7
	3	0.4	5.2	8.7	17.5
	4	0.3	4.0	8.1	16.2

The actual image enhancement effects of the four models are tested and the results are shown in Fig. 9, from which the enhanced image output by the proposed SIIP model has a better resolution performance, its fidelity is high, and the image has good expressiveness. The image output by ESRGAN model lacks some details. The image output by WDSR model has poor resolution and some details of the image are missing. The image output by BI model has serious distortion and very poor resolution performance.

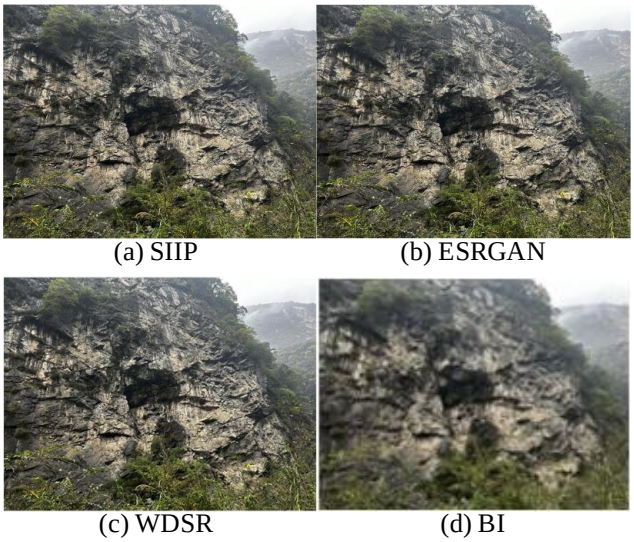

(a) SIIP (b) ESRGAN

(c) WDSR (d) BI

Fig. 9. Actual image enhancement tests of the four models.

V. RESULT AND DISCUSSION

Through experimental verification, the proposed sparse enhanced image processing model has shown excellent performance in image enhancement and super-resolution reconstruction tasks. In terms of PSNR and SSIM metrics, the average performance test results of this model on the DIV2k, Set5, and Set14 datasets are superior to the other three models, especially in image processing at high magnification, where the performance advantage of this model is more obvious. In addition, the response time of this model is significantly better than other models, and it has high processing efficiency. Meanwhile, the proposed sparse enhanced image processing model can better preserve image details and structural information during the image processing process, thereby achieving clearer and more accurate image restoration. Compared with existing methods, this model has higher performance and better robustness in image enhancement and super-resolution reconstruction tasks. By comparing the practical application effects of the four models, it can be found that the sparse enhanced image processing model proposed in this study has significant advantages in image quality and resolution. Compared with other models, this model can better solve the problems of blurring and distortion during image enlargement, achieving higher quality image output. In summary, the sparse enhanced image processing model proposed in the study has shown superior performance in image enhancement and super-resolution reconstruction tasks, providing effective image processing solutions for practical application scenarios. The efficiency, accuracy, and stability of this model in image processing make it widely applicable in practical applications.

VI. CONCLUSION

In the field of visual communication, image quality enhancement is crucial for the clarity and effectiveness of information delivery. Aiming at the limitations of existing image processing methods in quality enhancement, SIIP, an image processing model enhanced by sparsity, aims to improve the resolution and visual quality of images by reducing redundant information and enhancing the contribution of key pixels. A sparse coding technique based on deep learning is employed, and the SIIP model automatically learns the sparse representation during the training process to optimize the image reconstruction process. By comparing and analyzing with ESRGAN, WDSR and BI models, the SIIP model shows significant advantages. In the PSNR metric, the SIIP model reaches an average value of 32.9334 dB, which significantly outperforms the other models, with an improvement of 1.9252 dB compared to the closest model, ESRGAN. In the SSIM metric, the SIIP model also shows better structure preservation than the other models, and it also demonstrates better perceptual similarity in the LPIPS evaluation. In terms of response time, the SIIP model averages 0.82 seconds, which is much faster than the other compared models, including 18.30 seconds faster compared to the slowest BI model. These results of the SIIP model mark a significant advancement in the field of sparsity-enhanced image processing, which achieves an increase in the speed of image processing while maintaining a high level of fidelity. However, the computational complexity and real-time processing capability of the model are yet to be further optimized, especially in terms of performance scaling when processing higher resolution images. The real-time processing performance of the model should be further optimized in future research.

REFERENCES

[1] A. Geng, A. Moghiseh, C. Redenbach, and K. Schladitz, “Quantum image processing on real superconducting and trapped-ion based quantum computers,” TM-Tech. Mess, vol. 90, no. 7-8, pp. 445-454, May 2023.

[2] C. Cheng, B. Liu, F. Song, J. Jiang, Z. Li, and C. Song, et al., “An adaptive fuzzy logic control of green tea fixation process based on image processing technology,” Biosyst. Eng, vol. 215, no. 1, pp. 1-20, March 2022.

[3] P. C. Chen, C. Y. Cheng, and Y. S. Yang, "Displacement feedback control of actuators for structural testing using image processing and analysis," Earthq. Eng. Struct. D, vol. 51, no. 3, pp. 630-647, November 2022.

[4] R. Zeng, Y. Song, and L. V. Weizhen, "Dynamic modeling and damage analysis of debris cloud fragments produced by hypervelocity impacts via image processing," Front. Inform. Tech. El, vol. 23, no. 4, pp. 555-570, March 2022.

[5] G. Wu, T. Lin, W. Huo, and N. Cao, "Application of convolutional neural networks and image processing algorithms based on traffic video in vehicle taillight detection," Int. J. Sens. Netw, vol. 35, no. 3, pp. 181-192, March 2021.

[6] H. Cheng, K. H. Yap, and B. Wen, "Reconciliation of statistical and spatial sparsity for robust visual classification," Neurocomputing, vol. 529, no. 7, pp. 140-151, April 2023.

[7] J. Wang, V. Magron, and J. B. Lasserre, "TSSOS: A Moment-SOS hierarchy that exploits term sparsity," Siam. J. Optimiz, vol. 31, no. 1, pp. 30-58, January 2021.

[8] Y. Xue, W. Qin, C. Luo, P. Yang, and T. Niu, "Multi-Material decomposition for single energy CT using material sparsity constraint," IEEE. T. Med. Imaging, vol. 40, no. 5, pp. 1303-1318, May 2021.

[9] S. Anderson, C. White, and C. Farhat, "Space-local reduced-order bases for accelerating reduced-order models through sparsity," INT. J. Numer. Meth. Eng, vol. 124, no. 7, pp. 1646-1671, November 2023.

[10] Y. Wu, Y. Lan, L. Zhang, and Y. Xiang, "Feature flow regularization: improving structured sparsity in deep neural networks," Neural. Networks, vol. 161, no. 1, 598-613, April 2023.

[11] M. Zou, J. Yu, Y. Lv, B. Lu, W. Chi, and L. Sun, "A novel day-to-night obstacle detection method for excavators based on image enhancement and multisensor fusion," IEEE. Sens. J, vol. 23, no. 10, pp. 10825-10835, March 2023.

[12] Z. Tang, J. Wang, B. Yuan, H. Li, J. Zhang, and H. Wang, "Markov-GAN: Markov image enhancement method for malicious encrypted traffic classification," IET. Inform. Secur, vol. 16, no. 6, pp. 442-458, June 2022.

[13] J. Yang, Z. Guo, D. Zhang, B. Wu, and S. Du, "An anisotropic diffusion system with nonlinear time-delay structure tensor for image enhancement and segmentation," Comput. Math. Appl, vol. 107, no. 1, pp. 29-44, February 2022.

[14] G. Zhou, L. He, Y. Qi, M. Yang, X. Zhao, and Y. Chao, "An improved algorithm using weighted guided coefficient and union self-adaptive image enhancement for single image haze removal," IET. Image. Process, vol. 15, no. 11, pp. 2680-2692, May 2021.

[15] Y. Peng, Y. Yan, G. Chen, B. Feng, and X. Gao, "An underwater attenuation image enhancement method with adaptive color compensation and detail optimization," J. Supercomput, vol. 79, no. 2, pp. 1544-1570, July 2023.

[16] X. Song, J. Huang, J. Cao, and D. Song, "Feature spatial pyramid network for low-light image enhancement," Visual. Comput, vol. 39, no. 1, pp. 489-499, January 2023.

[17] K. Panetta, L. Kezebou, V. Oludare, and S. Again, "Comprehensive underwater object tracking benchmark dataset and underwater image enhancement with GAN," IEEE. J. Oceanic. Eng, vol. 47, no. 1, pp. 59-75, January 2022.

[18] Y. Li, Z. Yuan, K. Zheng, L. Jia, H. Guo, and H. Pan, "A novel detail weighted histogram equalization method for brightness preserving image enhancement based on partial statistic and global mapping model," IET. Image. Process, vol. 16, no. 12, pp. 3325-3341, June 2022.

[19] S. Pal, A. Roy, P. Shivakumara, and U. Pal, "Adapting a swin transformer for license plate number and text detection in drone images," AIA, vol. 1, no. 3, pp. 145-154, April 2023.

[20] S. Hao, Z. Wang, and F. Sun, "LEDet: A single-shot real-time object detector based on low-light image enhancement," Comput. J, vol. 64, no. 7, pp. 1028-1038, July 2021.